



Structure and Dynamics of Earth's Lower Mantle

Edward J. Garnero, *et al.*

Science **320**, 626 (2008);

DOI: 10.1126/science.1148028

The following resources related to this article are available online at www.sciencemag.org (this information is current as of May 12, 2008):

Updated information and services, including high-resolution figures, can be found in the online version of this article at:

<http://www.sciencemag.org/cgi/content/full/320/5876/626>

Supporting Online Material can be found at:

<http://www.sciencemag.org/cgi/content/full/320/5876/626/DC1>

This article **cites 39 articles**, 13 of which can be accessed for free:

<http://www.sciencemag.org/cgi/content/full/320/5876/626#otherarticles>

This article appears in the following **subject collections**:

Geochemistry, Geophysics

http://www.sciencemag.org/cgi/collection/geochem_phys

Information about obtaining **reprints** of this article or about obtaining **permission to reproduce this article** in whole or in part can be found at:

<http://www.sciencemag.org/about/permissions.dtl>

Structure and Dynamics of Earth's Lower Mantle

Edward J. Garnero* and Allen K. McNamara

Processes within the lowest several hundred kilometers of Earth's rocky mantle play a critical role in the evolution of the planet. Understanding Earth's lower mantle requires putting recent seismic and mineral physics discoveries into a self-consistent, geodynamically feasible context. Two nearly antipodal large low-shear-velocity provinces in the deep mantle likely represent chemically distinct and denser material. High-resolution seismological studies have revealed laterally varying seismic velocity discontinuities in the deepest few hundred kilometers, consistent with a phase transition from perovskite to post-perovskite. In the deepest tens of kilometers of the mantle, isolated pockets of ultralow seismic velocities may denote Earth's deepest magma chamber.

Earth's most profound internal boundary lies roughly halfway to its center, at a depth of nearly 2900 km, where the solid mantle meets the fluid outer core. Emerging research characterizes structure and processes on the mantle side of this boundary that influence chemistry and convection throughout the mantle, heat loss from the core, and Earth's thermal structure and evolution. The fields of seismology, mineral physics, geodynamics, and geochemistry have been key in providing new information. To better understand Earth's lowermost mantle, and hence whole-mantle processes, we summarize several recent observations and examine them in a geodynamical context.

Historically, the lowermost few hundred kilometers of the mantle was noted as having a reduced seismic velocity gradient with depth, interpreted as being caused by a lowermost-mantle thermal boundary layer above the hot core. This view was modified in the early 1980s, when seismologists observed a first-order discontinuous increase in velocity between 250 and 350 km above the core-mantle boundary (CMB) (1). This discontinuous jump is typically referred to as the D'' discontinuity. In the past few years, observations, modeling, and predictions have shown that the deepest mantle is complex (Fig. 1) and much more anomalous than the rest of the lower mantle. The term D'' is used to refer to the general depth shell of the lowermost several hundred kilometers of the mantle, and does not denote any specific structural characteristic.

Long-Wavelength Heterogeneity and Implications

Earth's internal structure is predominantly imaged by seismic methods. Tomographic inversions of seismic data yield maps of seismic-wave speed heterogeneity throughout the mantle, with a resolution typically greater than 1000 km (Fig. 1 and Fig. 2A). It has long been known that convergent

plate boundaries overlie regions of D'' with higher than average velocities, and that hot-spot volcanoes overlie regions with lower than average velocities. Such spatial correlations, combined with evidence for high P - and S -wave velocities mimicking slab shapes extending from beneath some subduction zones well into the lower mantle, constitute one argument in favor of whole-mantle convection (2, 3).

Seismic data suggest that two broad regions with lowered shear-wave speeds and higher than average density lie beneath the Pacific and Africa (4, 5). The African anomaly appears to extend upward from the CMB about 1000 km (6), whereas the height of the Pacific anomaly is less certain but probably at least 400 to 500 km. Each anomaly is about 15,000 km across, and together they cover nearly 50% of the CMB. The boundaries between these large low-shear-velocity provinces (LLSVPs) and normal mantle are sharp, as implied by seismic waves that graze LLSVP edges (6–8).

Geodynamic calculations show that chemically distinct deep-mantle regions can be formed and maintained, whereby mantle convection sweeps intrinsically denser material toward upwelling regions (9, 10) resembling LLSVP geometry (Fig. 2, A and B). This material must have intrinsic density elevated by a few percent relative to the surrounding mantle; if higher, structures would flatten out along the CMB, and if lower, they would be easily entrained in upwellings. If the resultant density is less than that of the surrounding mantle, the material is buoyant and forms large, doming structures that actively rise through the mantle (Fig. 2C). Alternatively, these thermochemical superplumes may heat up and rise because of excess thermal buoyancy, then cool and sink because of decreased thermal buoyancy (11). Smaller plumes that entrain some of the denser material can form on the tops of these structures. Assuming this behavior for Earth implies that LLSVPs are superplumes in various stages of ascent or fall (11).

If LLSVP thermal and compositional buoyancy are roughly balanced, then near-neutral or negative buoyancy can yield long-lived stable structures (9, 10, 12, 13). Piles are passively swept and shaped by mantle convection, preferentially accumulating into ridge-like structures beneath dominant upwelling centers (the Pacific and Africa). Plumes may originate from pile tops, particularly at peaks or ridges (Fig. 2B), and entrain nominal amounts of pile material. If the bulk modulus of pile material is anomalously high (e.g., consistent with subducted basaltic crust), structures intermediate to piles and superplumes can form, which have steeper sides than the other cases (13).

Lower-mantle chemical heterogeneity might also have existed since Earth's early differentiation. Seismic images of present-day structure would

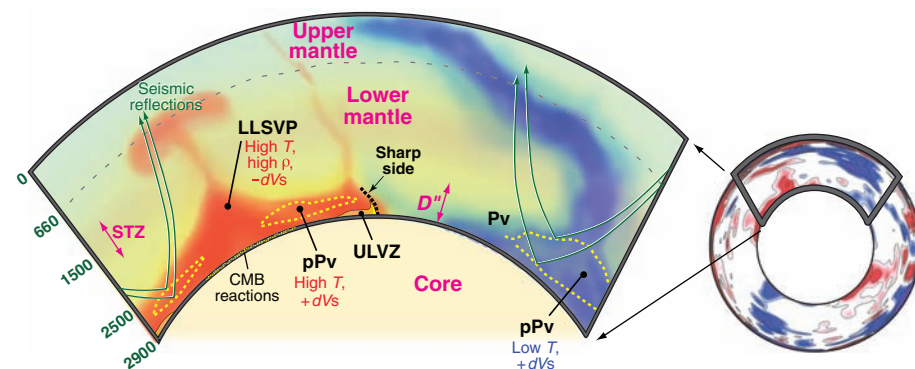


Fig. 1. Tomographically derived (43) high and low seismic velocity variations in Earth's mantle (blue and red, respectively) are shown in an equatorial cross section (right) viewed from the south, along with an enlarged panel (left) depicting several seismic findings in the D'' region. A large low-shear-velocity province (LLSVP) is found beneath the Pacific Ocean and Africa, and has high density (ρ) and temperature (T), with sharp sides between LLSVP low velocities ($-dVs$) and surrounding mantle. A pair of seismic reflectors seen beneath subduction as well as within the LLSVP is consistent with a double crossing of the perovskite (Pv) to post-perovskite (pPv) phase transition (yellow dashed lines), which locally elevates shear velocity ($+dVs$). Ultralow-velocity zone (ULVZ, yellow) material sits atop the CMB and can be swept around in lateral currents, possibly relating to chemical reactions between the mantle and core. The spin transition zone (STZ) centered near 1500 km depth represents a change in the spin state of Fe^{2+} to Fe^{3+} and may also affect lower-mantle densities and velocities (44, 45).

School of Earth and Space Exploration, Arizona State University, Box 871404, Tempe, AZ 85287, USA.

*To whom correspondence should be addressed. E-mail: garnero@asu.edu

thus depict remnants of this material, which may be slowly entraining away through time. Alternatively, denser material might have accumulated throughout Earth's history and might consist of chemical reaction products from the CMB (14) or subducted oceanic crust (13, 15, 16). Piles composed of a long-lived primordial layer will likely have sharp contacts at their top surface (Fig. 2B), whereas those composed of accumulated subducted crust may have a rough or diffusive top (Fig. 2D).

Geodynamic models predict that superplumes have doming, concave-downward tops; piles, on the other hand, have concave-upward tops surrounded by ridges. A velocity reduction some 300 to 400 km above the CMB is imaged in the central Pacific (17) and may represent the top of the Pacific pile. Improving the resolution of the

present beneath subduction in high-velocity regions as well as within the low-velocity LLSVPs, with geographical variation of the depth and velocity change across the discontinuity. However, deep-mantle discontinuities have been studied in detail in only a few isolated regions, and much of the CMB is still unmapped. Only a handful of earthquake-to-receiver geometries produce seismic data that allow this feature to be probed and mapped. Two regions have attracted researchers: (i) beneath the Cocos Plate, Central America, and the Caribbean, a region underlying long-lived subduction; and (ii) beneath the central Pacific, a region beneath presumed upwelling and within the Pacific LLSVP. These locations take advantage of the two most prolific deep-focus earthquake zones: Fiji-Tonga and

of *P* waves have been less common than for *S* and typically lack clear waveform evidence for *D''* reflections, although there are some exceptions (24). More commonly, stacking of hundreds or thousands of seismograms is necessary to detect reflected *P*-wave energy (25); thus, the discontinuity is a much weaker reflector for *P* waves.

Lateral variations in deep-mantle temperature are expected but should be smooth, and hence they do not explain a step velocity increase associated with the *D''* discontinuity, nor differing *S*- and *P*-wave discontinuity strengths. Furthermore, numerical models predict that lowermost-mantle thermal boundary layers should be thin, much less than the observed discontinuity height. Thus, *D''* has been variously interpreted as chemical dregs from subduction, as a region of chemical reaction between the core and mantle, as a boundary between isotropic and anisotropic fabrics, or as a solid-state phase change (26). Recently, the latter hypothesis has gained favor, owing to the recent discovery of an exothermic phase transition in deep-mantle perovskite (Pv) to a post-perovskite (pPv) structure (27–29).

If this phase transition is responsible for the *D''* discontinuity in cold, high-velocity regions, then the experimentally determined positive Clapeyron slope of the transition predicts that the discontinuity should deepen or even vanish in hot areas. However, clear evidence is present for an *S*-wave discontinuity within the Pacific LLSVP (17), with height above the CMB and topographical variability both similar to the region beneath the Cocos Plate. This supports the idea that LLSVPs may have a different mantle composition (perhaps increased iron abundance) that perturbs the phase boundary depth. However, some form of chemical stratification could also generate reflections in the LLSVP.

Because temperature is expected to strongly increase with depth near the hotter outer core, post-perovskite may revert back to perovskite closer to the CMB, depending on Clapeyron slope and temperature. Thus, a lens of post-perovskite is possible from a double crossing of the phase boundary (30). Attributing a pair of seismically detected *D''* discontinuities (i.e., a velocity increase overlying a decrease) to post-perovskite permits determination of temperature at the two discontinuity depths, if thermal conductivity and Clapeyron slope are known. In turn, this permits estimation of core heat flux of 50 to 100 mW/m² (17, 23), a range of values much higher than estimates based on plume buoyancy flux. Although the phase transition is not expected to greatly alter first-order dynamics, an exothermic phase change at these depths could enhance the generation of plumes, affecting CMB heat flow (31). A lower CMB temperature would preclude the double crossing.

Accurate characterization of the deeper discontinuity is challenging because *P*- and *S*-wave reflections from a discontinuous velocity reduction at the magnitude predicted by mineral physics

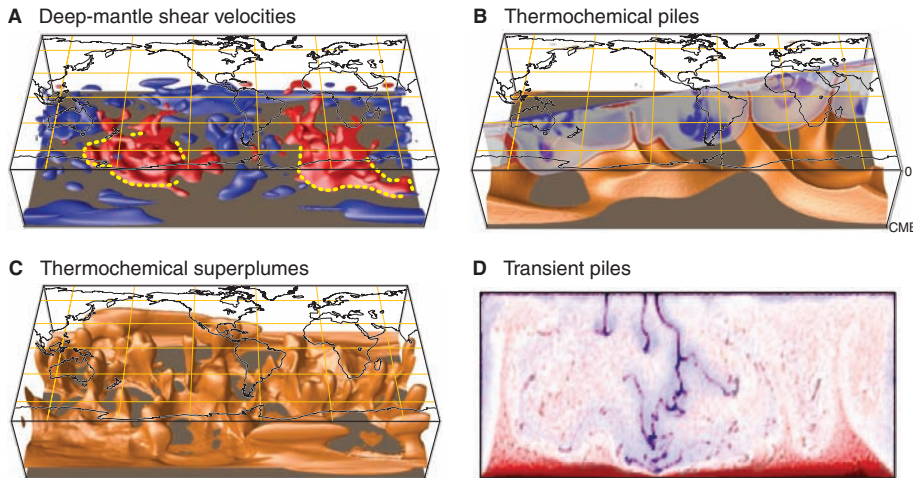


Fig. 2. (A) Shear velocity perturbations between 660 km depth and the CMB, isocontoured at $\pm 0.6\%$ (blue/red) for model S20RTS (43). Sharp LLSVP edges (yellow dashed lines) have been noted for both LLSVPs (8). (B to D) Geodynamical modeling results illustrating different conceptual models to explain LLSVPs observed beneath Africa and the Pacific (see supporting online text for details of calculations). All calculations extend from the CMB to the surface, and the 3D calculations are performed in spherical geometry, unwrapped into a box for easier visualization. (B) 3D thermochemical piles (gold), shown with a whole-mantle temperature cross section (red and blue denote hot and cold, respectively). (C) 3D thermochemical superplumes (gold). (D) 2D calculations of transient thermochemical piles created by accumulated subducted crust, with temperature and composition superimposed (red/blue = hot/cold; denser material is darker).

sharpness and variability of this reduction will assist in constraining LLSVP origin and evolution.

The trace chemistry of ocean-island basalts (OIBs), if from a deep-mantle origin, may shed light on LLSVP chemistry. Volcanic hot spots tend to overlie LLSVP edges rather than their interiors (18), which is consistent with edges and ridges of thermochemical piles forming in regions of return flow and initiating plumes (9, 10). Efforts to directly image plumes are encouraging (19) but controversial (20). Numerical models of mantle convection show that plume morphologies are often more complicated than simple vertically continuous whole-mantle conduits (e.g., bent and curved central conduits, complicated plume head shapes, thin or diminishing plume tails, etc.).

Regional *D''* Studies

Evidence for a shear-wave velocity discontinuity at the top of *D''* is unequivocal. It is

South America, and dense seismic networks in North America.

Typically, attributes of seismic-wave reflectance are extracted throughout some volume of interest by stacking or summing seismic records. These data permit mapping of lateral variations in *D''* discontinuity height above the CMB. For example, a 100-km vertical offset in *D''* discontinuity depth is observed beneath the Cocos plate (21, 22). A second, deeper reflector is evident in some studies beneath the velocity increase, mapped as a velocity reduction (21–23). Beneath the central Pacific, up to four discontinuities in the shear velocity have been detected (17). A major uncertainty in interpreting the seismic data is the assumption of a reference velocity structure. For example, lateral variations in the height of the *D''* discontinuity, underlain by constant velocity, can trade off with a model containing a fixed height but underlain with variations in velocity. Studies

studies (32) should be weak (33). Also, small-scale heterogeneity may complicate the detection of the lower boundary by scattering energy (22). Another challenge is that the *P*-wave jump associated with the entrance into the pPv phase is predicted to be small and negligible—fractions of a percent, and possibly even negative (32).

Horizontal and vertical components of shear waves with appreciable path lengths in the deepest mantle have slightly different arrival times for some regions, indicating seismic anisotropy in *D''*. Anisotropy is detected beneath implied downwelling flow (e.g., beneath the Caribbean, Alaska, and Eurasia) and upwelling (e.g., beneath the central Pacific) and has been suggested to be weak outside these regions (34, 35). Most data imply that the orientation of anisotropy is three-dimensional, with shear-wave splitting depending on azimuth. If the link between observations and dynamical predictions can be properly established, it may be possible to provide constraints on mantle flow patterns and rheology of the lowermost mantle (36). The main minerals in the lower mantle—Pv, pPv, and magnesiowüstite—are each strongly anisotropic but may respond differently to deformation, which makes inference of mantle flow patterns from observed anisotropy more difficult.

As Pv transforms to pPv, preexisting fabric undergoing transition is expected to be severely altered, and perhaps erased, by the major change in crystal structure; however, preexisting fabrics in magnesiowüstite should remain and combine with developing fabric in the new pPv grains at greater depths. An additional complication is that magnesiowüstite and pPv likely have different rheologies, such that the weaker of the two minerals may accommodate much more deformation [hence, more lattice-preferred orientation (LPO)] than the stronger mineral. If pPv is the cause of the *D''* discontinuity and is also the dominant mineral associated with *D''* anisotropy, then there may be an offset between the depths of the discontinuity and the onset of anisotropy, because some finite amount of deformation is required to develop LPO in pPv (fig. S3). This may explain seismic observations under the central Atlantic, thought to be away from current downwellings, in which there is evidence for a *D''* discontinuity (37) but only weak (or absent) seismic anisotropy (35).

Ultralow-Velocity Zones

Thin patches (5 to 40 km thick) in which *P*- and *S*-wave velocities are reduced by up to 10% and 30%, respectively, have been imaged directly above the CMB in several places (38). These characteristics are consistent with the presence of some melt in the lowermost mantle (39). An ultralow-velocity zone (ULVZ) density increase of up to 10% has also been noted (40). If the origin of the ULVZs is partial melt, they should be present wherever rock of appropriate composition exists, because the CMB is isothermal. However, ULVZs should be thickest in the hottest regions above the CMB. Modeling implies that these regions are at the base of

plumes in an isochemical mantle, which would correspond to the center of LLSVPs (fig. S4A). However, if LLSVPs are thermochemical structures, the hottest regions should be at their edges (8, 9, 13). Several studies show evidence for ULVZ structure near the edge of the Pacific LLSVP (17, 40), consistent with it being a thermochemical structure (fig. S4B). Assessing the geometry and extent of ULVZs is challenging because their thickness may drop below the limits of seismic detection. Thin ULVZs having only mild velocity drops are even harder to detect.

Other mechanisms that produce ULVZ material are chemical heterogeneity from the mantle chemically reacting with the core (14) and CMB underside sedimentation (41). However, the 3-to-1 ratio of *S*-to-*P* velocity reduction likely requires some degree of partial melting. An interesting possibility involves pPv: If the deepest mantle is cool enough to avoid a double crossing of the pPv phase boundary, iron-rich pPv can explain an ULVZ layer (42). However, recent work imaged both a double crossing of the pPv phase boundary and a deeper ULVZ layer in the Pacific (14). For a chemical and/or partial-melt origin, episodic entrainment of ULVZ material may be possible (8), leading to heterogeneities throughout the *D''* layer in certain regions. Viscous convective forces may be strong enough that even high-density (>10%) material can be swept either to the base of plumes or to the edges of chemically distinct piles.

Next Steps

Seismological studies reveal a lowermost mantle rich in complexity on a variety of spatial scales: the large LLSVPs beneath Africa and the Pacific, the regionally variable *D''* discontinuities observed ~200 to 300 km above the CMB, and isolated ULVZs in the lowermost tens of kilometers of the mantle. Mineral physics experiments imply that heterogeneities in temperature, composition, and phase are required to explain seismic observations. Several geodynamic hypotheses have arisen to explain these observations in the context of larger-scale mantle convection. Increased collaboration among disciplines involved in deep Earth interior research will be helpful in resolving the fundamental questions that remain.

References and Notes

1. T. Lay, D. V. Helmberger, *Geophys. J. R. Astron. Soc.* **75**, 799 (1983).
2. R. D. van der Hilst, S. Widiyantoro, E. R. Engdahl, *Nature* **386**, 578 (1997).
3. S. P. Grand, R. D. van der Hilst, S. Widiyantoro, *GSA Today* **7**, 1 (1997).
4. J. Trampert, F. Deschamps, J. Resovsky, D. A. Yuen, *Science* **306**, 853 (2004).
5. M. Ishii, J. Tromp, *Phys. Earth Planet. Int.* **146**, 113 (2004).
6. S. Ni, E. Tan, M. Gurnis, D. V. Helmberger, *Science* **296**, 1850 (2002).
7. Y. Wang, L. Wen, *J. Geophys. Res.* **112**, B05313 (2007).
8. E. J. Garnero, T. Lay, A. K. McNamara, in *The Origin of Melting Anomalies: Plates, Plumes and Planetary Processes*, G. R. Foulger, D. M. Jurdy, Eds. (Geological Society of America, Boulder, CO, 2007), pp. 79–102.
9. A. K. McNamara, S. Zhong, *Nature* **437**, 1136 (2005).

10. P. J. Tackley, *Geochem. Geophys. Geosyst.* **3**, 10.1029/2001GC000167 (2002).
11. A. Davaille, E. Stutzmann, G. Silveira, J. Besse, V. Courtillot, *Earth Planet. Sci. Lett.* **239**, 233 (2005).
12. A. M. Jellinek, M. Manga, *Rev. Geophys.* **42**, RG3002 (2004).
13. E. Tan, M. Gurnis, *Geophys. Res. Lett.* **32**, L20307 (2005).
14. E. Knittle, R. Jeanloz, *Science* **251**, 1438 (1991).
15. U. R. Christensen, A. W. Hofmann, *J. Geophys. Res.* **99**, 19867 (1994).
16. K. Hirose, N. Takafuji, N. Sata, Y. Ohishi, *Earth Planet. Sci. Lett.* **237**, 239 (2005).
17. T. Lay, J. Hernlund, E. J. Garnero, M. S. Thorne, *Science* **314**, 1272 (2006).
18. M. Thorne, E. J. Garnero, S. Grand, *Phys. Earth Planet. Int.* **146**, 47 (2004).
19. R. Montelli *et al.*, *Science* **303**, 338 (2004); published online 4 December 2003 (10.1126/science.1092485).
20. R. D. van der Hilst, M. V. De Hoop, *Geophys. J. Int.* **167**, 1211 (2006).
21. C. Thomas, E. J. Garnero, T. Lay, *J. Geophys. Res.* **109**, 10.1029/2004JB003013 (2004).
22. A. Hutko, T. Lay, E. J. Garnero, J. S. Revenaugh, *Nature* **441**, 333 (2006).
23. R. D. van der Hilst *et al.*, *Science* **315**, 1813 (2007).
24. M. Weber, J. P. Davis, *Geophys. J. Int.* **102**, 231 (1990).
25. T. Kito, S. Rost, C. Thomas, E. J. Garnero, *Geophys. J. Int.* **169**, 631 (2007).
26. M. Wyssession *et al.*, in *The Core-Mantle Boundary Region*, M. Gurnis, M. Wyssession, E. Knittle, B. Buffett, Eds. (American Geophysical Union, Washington, DC, 1998), pp. 273–298.
27. M. Murakami, K. Hirose, K. Kawamura, N. Sata, Y. Ohishi, *Science* **304**, 855 (2004); published online 8 April 2004 (10.1126/science.1095932).
28. A. R. Oganov, S. Ono, *Nature* **430**, 445 (2004).
29. T. Tsuchiya, J. Tsuchiya, K. Umemoto, R. M. Wentzcovitch, *Earth Planet. Sci. Lett.* **224**, 241 (2004).
30. J. W. Hernlund, C. Thomas, P. J. Tackley, *Nature* **434**, 882 (2005).
31. T. Nakagawa, P. J. Tackley, *Geophys. Res. Lett.* **31**, L16611 (2004).
32. J. Wookey, S. Stackhouse, J.-M. Kendall, J. Brodholt, G. D. Price, *Nature* **438**, 1004 (2005).
33. T. Lay, E. J. Garnero, in *Post-Perovskite: The Last Mantle Phase Transition*, K. Hirose, D. Yuen, T. Lay, J. Brodholt, Eds. (American Geophysical Union, Washington, DC, 2007), pp. 129–154.
34. T. Lay *et al.*, in *The Core-Mantle Boundary Region*, M. Gurnis, M. Wyssession, E. Knittle, B. Buffett, Eds. (American Geophysical Union, Washington, DC, 1998), pp. 299–318.
35. E. J. Garnero, M. M. Moore, T. Lay, M. J. Fouch, *J. Geophys. Res.* **109**, 10.1029/2004JB003004 (2004).
36. S. Merkel *et al.*, *Science* **316**, 1729 (2007).
37. M. Wallace, C. Thomas, *Phys. Earth Planet. Int.* **151**, 115 (2005).
38. M. S. Thorne, E. J. Garnero, *J. Geophys. Res.* **109**, B08301 (2004).
39. Q. Williams, E. J. Garnero, *Science* **273**, 1528 (1996).
40. S. Rost, E. J. Garnero, Q. Williams, M. Manga, *Nature* **435**, 666 (2005).
41. B. A. Buffett, E. J. Garnero, R. Jeanloz, *Science* **290**, 1338 (2000).
42. W. L. Mao *et al.*, *Science* **312**, 564 (2006).
43. J. Ritsema, H. J. van Heist, J. H. Woodhouse, *J. Geophys. Res.* **109**, B02302 (2004).
44. J. Badro *et al.*, *Science* **305**, 383 (2004).
45. J.-F. Lin *et al.*, *Science* **317**, 1740 (2007).
46. We thank J. Ritsema for the tomographic model. Supported by NSF grants EAR-0711401 and EAR-0453944 (E.J.G.) and by NSF grants EAR-0510383 and EAR-0456356 (A.K.M.).

Supporting Online Material

www.sciencemag.org/cgi/content/full/320/5876/626/DC1
SOM Text
Figs. S1 to S5
Table S1
References
10.1126/science.1148028